Supplementary information
Deeply nonlinear excitation of self-normalised exchange spin waves

Qi Wang[1,2,3], Roman Verba[4], Björn Heinz[5], Michael Schneider[5], Ondřej Wojewoda[6], Kristyna Davidkova[6], Khrystyna Levchenko[1], Carsten Dubs[7], Norbert J. Mauser[2,3], Michal Urbánek[6], Philipp Pirro[5], Andrii V. Chumak[1,2]

[1] *Faculty of Physics, University of Vienna, Vienna, Austria*

[2] *Research Platform Mathematics-Magnetism-Materials, c/o Faculty of Math, University of Vienna, Vienna, Austria*

[3] *Wolfgang Pauli Institute, Vienna, Austria*

[4] *Institute of Magnetism, Kyiv, Ukraine*

[5] *Fachbereich Physik and Landesforschungszentrum OPTIMAS, Technische Universität Kaiserslautern, Kaiserslautern, Germany*

[6] *CEITEC BUT, Brno University of Technology, Brno, Czech Republic*

[7] *INNOVENT e.V., Technologieentwicklung, Jena, Germany*

In the supplementary information, Section 1 discusses the comparisons between the simulated dispersion curves, the classical spin-wave dispersion curve theory and the semianalytical theory. In Section 2, the simulated spin-wave intensity as a function of excitation frequency is presented. In Section 3, the influence of the Joule heating on the nonlinear frequency shift is discussed. The contribution of nonlinearity to the energy conversion from FMR mode to exchange spin waves is discussed in Section 4.

1. Forward volume spin waves dispersion curve in nanoscale waveguides

Dispersion characteristic is fundamental information for magnonic studies. The dipole-exchange spin-wave spectrum theory for ferromagnetic films, developed by Kalinikos and Slavin, is a classical theory which has been widely used in the calculation of the dispersion curve in macro/micro-scale waveguides [S1]. However, this theory was developed with a uniform static demagnetisation field approximation, which is not applicable to the nanoscale waveguides with nonuniform internal field in our studies. Here, we present a semianalytical theory that accounts for the nonuniform static demagnetisation field. This nonuniformity leads to partial pinning of spin waves at the lateral edges of waveguide and changes the propagation characteristics of spin waves, i.e., the dispersion curve. Figure 1 shows the comparison between the simulated dispersion curve (colormap), the classical theory (red line) and the presented semianalytical theory (black dashed line). The parameters of simulation and calculation are the same as those used in the main text. It can be clearly seen that the semianalytical theory (black dashed line) was able to well reproduce the simulated results. However, there is a discrepancy between the classical theory (red line) and simulated dispersion curve (colormap). Therefore, the nonuniformity has to be considered during the calculation of dispersion curve for the nanoscale waveguides. Furthermore, the simulated dispersion curves also show that the higher width modes have been pushed up significantly in frequency due to waveguide's nanoscale width and large exchange contribution.

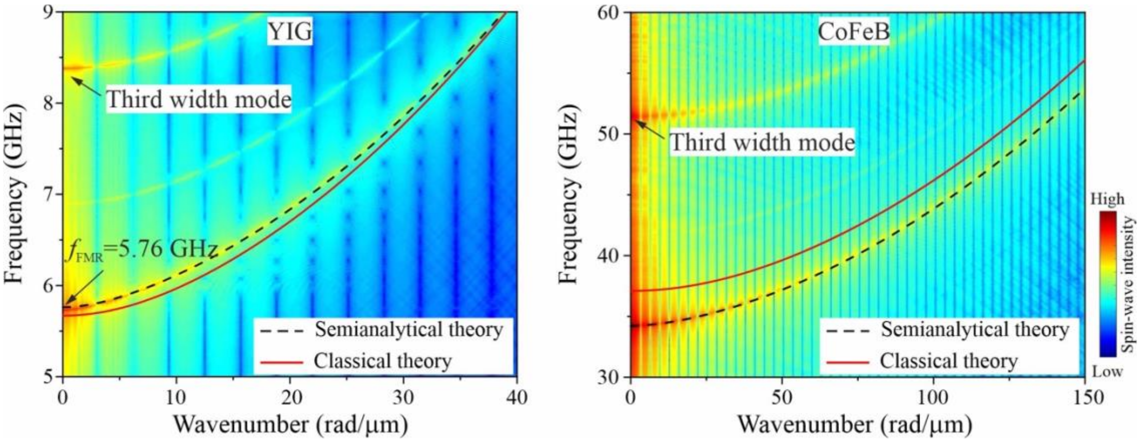

Fig. S1 Simulated dispersion curves (colormap) of (a) a 200 nm wide 44 nm thick YIG waveguide with 330 mT out-of-plane magnetic field and (b) a 50 nm wide 5 nm thick CoFeB waveguide with 2.55 T out-of-plane magnetic field. The red solid line and black dashed line represent the classical theory prediction and the semianalytical theory.

2. Simulated spin-wave intensity as a function of excitation frequency

In the main text, we attribute the decrease in the BLS intensity in the high-frequency range (above 6.4 GHz) to the reduced detection efficiency of μBLS for short wavelengths. To verify this, we performed micromagnetic simulations similar to the experiments, where the excitation frequency sweeps from 5.6 GHz to 7 GHz (or vice versa) with a step size of 20 MHz. Figure S2 shows the simulated spin-wave spectra with similar foldover and bistability behaviour. More importantly, the simulated spin-wave intensity increases monotonically with the increase of frequency, which confirming our statement in the main text that the decrease in the BLS intensity in the high-frequency range is due to the decrease of the detection efficiency of μBLS for short wavelengths.

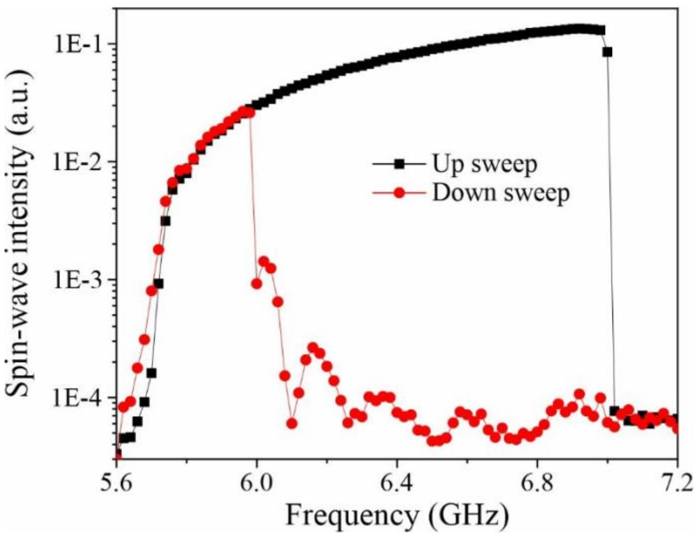

Fig. S2 Simulated spin-wave intensity as a function of excitation for up- and down-frequency sweep.

3. The influence of Joule heating on nonlinear frequency shift

In Fig. 3(a) of the main text, a large frequency shift is observed by using continuous wave (CW) excitations. To investigate the effect of the Joule heating produced by the microwave current on the frequency shift, pulse excitations with different duration times are used. The power and repetition time of the pulse are fixed at 12 dBm and 1000 ns, respectively. The pulse duration varies from 900 ns to 300 ns as shown in Fig. S3. The black dot line shows the reference signal obtained by down-sweep CW excitation (from high frequency to low frequency). In all cases, a clear frequency jump point is observed, which is a good "sensor" for estimating the influence of the Joule heating. The frequency of the jump point slightly decreases by 20 MHz from 5.79 GHz (CW) to 5.75 GHz (300 ns pulse). The contribution of Joule heating to the frequency shift can be neglected compared to the total frequency shift of 2.1 GHz. Therefore, the frequency shift obtained in the main text is mainly due to the nonlinear phenomena.

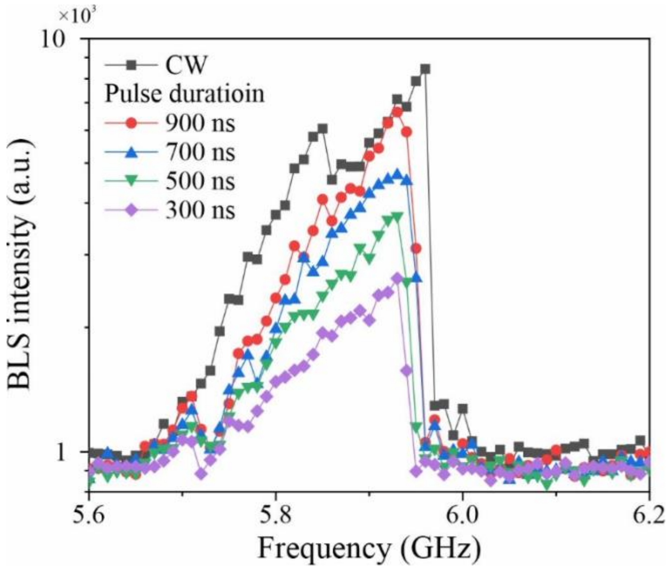

Fig. S3 The μBLS intensity as a function of excitation frequency for continue wave (black dot line) and pulse excitation with different pulse durations.

4. The contribution of nonlinearity for the energy conversion

In the main text, the energy conversion from FMR mode to exchange spin waves is estimated to be more than 80% by calculating the power of propagating spin waves and the power dissipated under the antenna region. To verify the contribution of the nonlinearity to the energy conversion process, a spatial modulated external field is constructed and inserted into Mumax3 to simulate the wavenumber conversion in the linear case.

Firstly, we take the internal field from Fig. 3(a) and increase it by ~130 mT to compensate for the demagnetisation field, and plug it into Mumax^3 as a spatial modulated external field. In this case, the FMR frequency under the antenna is around 7.55 GHz in the linear region. The top panel of Fig. S4 shows the spatial dependent internal field extracted from Mumax^3. Secondly, a very small Oersted field generated by the 2 μm antenna is used to excite the linear spin waves with precession angles below 1°. The middle panel of Fig. S4 shows the snapshot of the simulated spin-wave amplitude m_x as a function of propagation distance in the waveguide. The bottom panel shows the precession angle as a function of the propagation distance, where most of the energies are concentrated under the antenna. A similar wavelength conversion from FMR mode to exchange waves is observed, but with lower energy conversion efficiency. Table S1 summarized of the energy transmission estimated using the way mentioned in the Methods. It shows that the energy transmission ratio T_R is 83% for nonlinear case and 55% for linear case. If we compare the parasitic losses, i.e., $L_p = 1 - T_R$, the nonlinear mechanism is around 2.6 times more efficient than linear one. Finally, in the main text, we concluded that despite the similarity, such conversion is much less efficient when the spin-wave dispersion shift is determined not by nonlinearity, but by spatial modulation of the external field or magnetic parameters, since a spin-wave is partially reflected from such a sharp boundary.

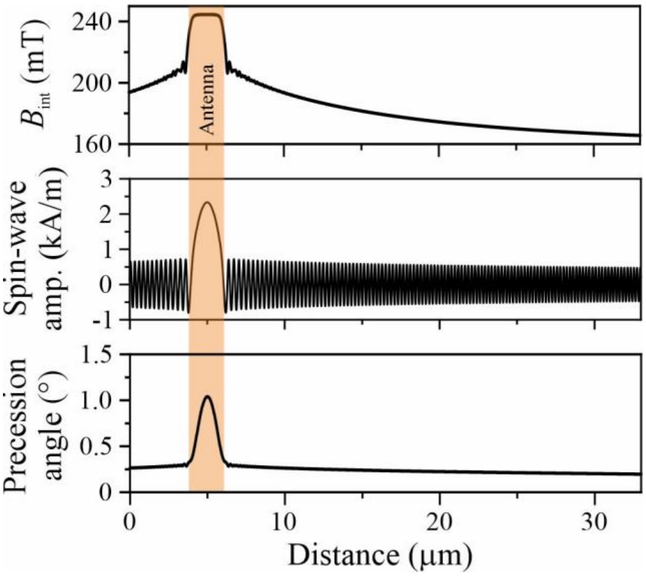

Fig. S4 The internal field (top panel), the spin-wave amplitude (middle panel), and the precession angle (bottom panel) as a function of distance for linear excitation.

Table S1. The summary of the energy transmission

	Averaged SW energy density under antenna $\langle W_{sw} \rangle$ (J/m^3)	SW energy density close to antenna (at 500 nm distance) $\langle W_{sw} \rangle$ (J/m^3)	v_g (m/s)	PG	$2P_{sw}$	T_R %
Nonlinear case	15591	10270	348	13 nw	63 nW	83
Linear case	3.61	0.53	408	3.1 pW	3.8 pW	55

Supplementary References:

S1. Kalinikos, B. A. & Slavin, A. N. Theory of dipole-exchange spin wave spectrum for ferromagnetic films with mixed exchange boundary conditions. *J. Phys. C: Solid Phys.* **19**, 7013 (1986)